Author Accepted Manuscript version of the paper by Stefanakos, C., De Vaal, J. B., & Dos Santos Sousa Rodrigues, J. M. (2023). Investigation of the feasibility for a combined offshore wind and wave energy plant in the Norwegian waters. Proceedings of the 33rd International Ocean and Polar Engineering Conference, Ottawa, Canada, June 19-23, 2023 - ISOPE 2023, 33. https://onepetro.org/ISOPEIOPEC/proceedings-abstract/ISOPE23/All-ISOPE23/ISOPE-I-23-107/524436.

Investigation of the feasibility for a combined offshore wind and wave energy plant in the Norwegian waters

Christos Stefanakos[1], *Jacobus de Vaal*[2], *José Miguel Rodrigues*[2]
[1]SINTEF Ocean, Fisheries and New Biomarine Industry, Trondheim, Norway
[2]SINTEF Ocean, Ships and Ocean Structures, Trondheim, Norway

ABSTRACT

Offshore areas in Norwegian waters with negative correlation between wind and wave energy resources have been identified. This finding is of great importance, as it suggests that combined wind and wave energy deployment sites may be particularly efficient, as they provide a prolonged effective period of use with high energy absorption which would otherwise not be possible. This comes with the additional economic advantage of concurrent location in terms of installation and access for maintenance. In the present study, co-located wind and wave farms are considered at different sites with varying wind-wave correlations. Metrics such as the Annual Energy Production (AEP) and Mean Annual Energy Production (MAEP), and their variation during a year are analyzed. Different wind/wave energy converter designs with published power matrices are used for estimating the absorbed power, as well as other relevant metrics, throughout the entire period covered by the ERA5 database. A methodology is proposed for easily assessing the potential of new marine wind and wave renewable devices at early stages of development, covering areas of the Norwegian coastal zone, and using real climate data.

KEY WORDS: offshore wind power; wave power; ERA5; probability analysis; Annual Energy Production; Norway

INTRODUCTION

Following Cozzi et al. (2022), electricity use based on renewable energy grew to 26.2 % (2019), bringing the share of renewables in global electricity consumption to the fifth place of Total Final Energy Consumption (TFEC) in 2019. Hydropower remains by far the largest source of renewable electricity globally, followed by wind and solar PV.

Lately, the combination of offshore wind and wave energy has attracted the interest of both academic and industrial world; see, e.g., Pérez-Collazo et al. (2015); McTiernan and Sharman (2020).

There are various synergies in this combination that could potentially lead to benefits both in the technological domain (common grid infrastructure, shared logistics, common mooring or foundation systems, shadow effects) and the generation process (enhanced energy harvest, smoother power output,reduction in sudden grid disconnections, reduced number of hours of non-activity, more accurate output forecast) (Rosa-Santos et al., 2022).

Especially, for the reduction in power output variability, Astariz and Iglesias (2016a,b) have found reductions in downtime and power variability for the North Sea Alpha Ventus and Horns Rev offshore wind farms of approximately 87 and 6%, respectively, due to the presence of co-located wave farms. In addition, Gaughan and Fitzgerald (2020) found that, in the Irish West coast, the power variability of offshore wind farms could be significantly reduced by the co-location of wave energy farms.

Furthermore, Astariz and Iglesias (2016a,b) found that the sheltering effect of co-located wave farms could increase up to 20% the annual accessibility to offshore wind farms located in the North Sea.

In a previous resource assessment study (Stefanakos et al., 2021), offshore areas in the Norwegian waters with negative correlation between wind and wave energy resources had been identified. This finding is of great importance, as it suggests that combined wind and wave energy deployment sites may be particularly efficient, as it is mentioned above, providing a prolonged effective period of use with high energy absorption.

In the present work, an academic case-study scenario has been developed of a potential combined wind and wave farm at a location selected with respect to various criteria; such as wind and wave power resource availability, closeness to the shore and/or conflicts with other marine activities.

Metrics such as the yearly absorbed power and its annual variation have been analyzed. Different wind/wave energy converter types with published/state-of-the-art power matrices have been used for the estimation of hourly absorbed energy throughout the entire period covered by the ERA5 database.

The described procedure would potentially establish a working methodology for easily assessing the potential of marine wind and wave renewable devices at early stages of development.

EVALUATION OF WAVE AND WIND POWER RESOURCE

Data Used

For the resource evaluation of offshore wind and wave power, ECMWF's wind and wave database ERA5 is used (Hersbach et al., 2020), which covers 40 years (1979-2019) in 1-hr intervals. It is also worth-noticing the direct use of mean energy period and wind speed at 100 m height for the first time, instead of using empirical approximations based on relations with peak period and wind speed at 10 m, respectively.

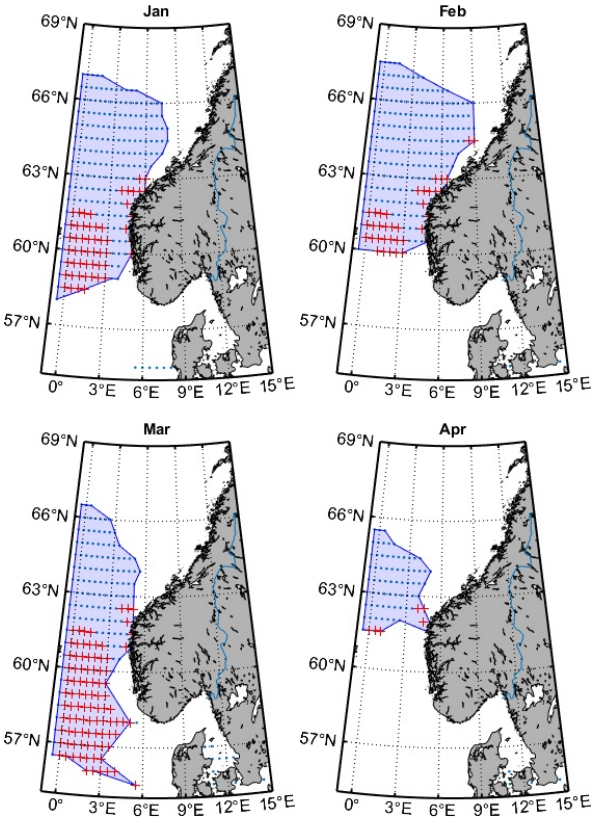

Fig. 1. Areas with negative correlation, Jan-Apr (red '+': <200 m depth)

Areas with negative correlation

Following the analysis in Stefanakos et al. (2021), the correlation between wave and wind power can be studied by means of the Pearson's correlation coefficient R (1 stands for wave, and 2 for wind):

$$R_{X_1X_2} = \frac{\overline{X_1\,X_2} - \overline{X_1}\;\;\overline{X_2}}{\sqrt{\left(\overline{X_1^2} - \overline{X_1}^2\right)\left(\overline{X_2^2} - \overline{X_2}^2\right)}}, \tag{1}$$

where $\overline{X}$ are appropriate mean values (over years, months, etc).

Indicator $R_{X_1X_2}$ ranges from -1 to 1, where positive values indicate positive correlation, i.e. high (resp. low) values of wave are correlated with high (resp. low) values of wind power. Conversely, negative values indicate negative correlation, i.e. high (resp. low) values of wave power are correlated with low (resp. high) values of wind power. For the negative correlation, see also discussion for Figs. 8–9 in p. 7.

Following definition 1, the monthly variability of wind and wave power data with negative correlation in the southern part of Norway is investigated; see Figs. 1–3. The identified area is quite large during the winter months, when the electricity consumption is higher, while it remains active even in months with low demand like August. Hence, this fact can be further exploited by considering the installation of hybrid solutions.

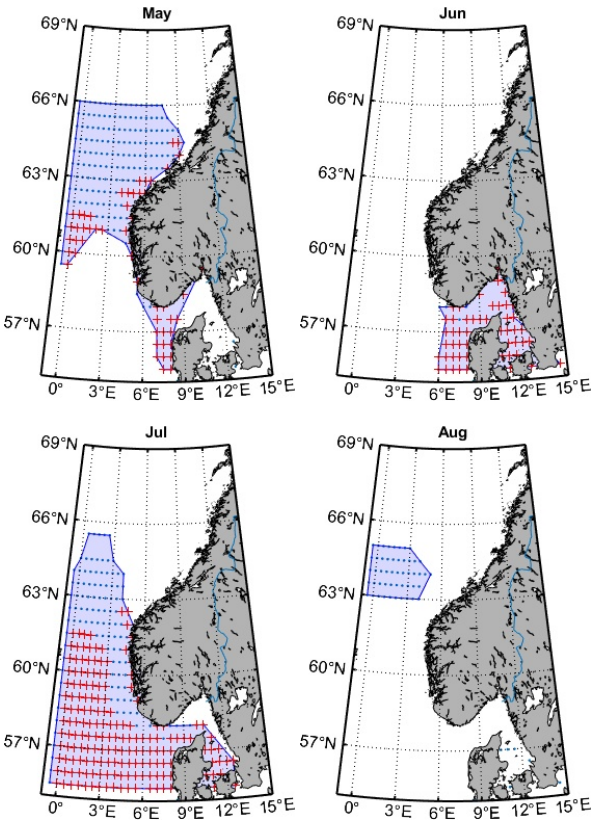

Fig. 2. Areas with negative correlation, May-Aug (red '+': <200 m depth)

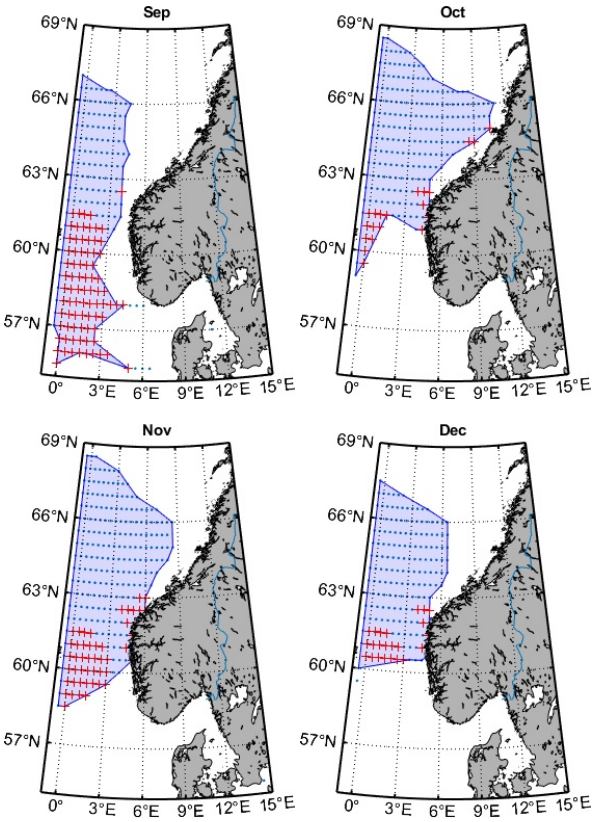

Fig. 3. Areas with negative correlation, Sep-Dec (red '+': <200 m depth)

Table 1. Points with negative correlation

Point	Lat (N)	Lon (E)	Depth (m)
103	62.5	4.0	182
111	62.5	4.5	200
112	62.0	4.5	161
113	61.0	4.5	107
121	62.5	5.0	175
122	61.5	5.0	31
123	60.5	5.0	175
124	60.0	5.0	107
133	63.0	5.5	133
134	62.5	5.5	133
142	63.0	6.0	189
143	62.5	6.0	24
151	63.0	6.5	79
173	63.5	8.0	19
181	64.5	8.5	156
184	64.5	9.0	200
185	64.0	9.0	104
195	65.0	10.5	193

Table 2. Mean monthly variability of wave power (kW/m)

	103	111	112	113	121	122
Jan	82.09	74.27	66.80	42.51	55.18	12.71
Feb	72.01	65.86	58.64	35.36	49.44	11.05
Mar	57.72	52.87	47.16	28.48	39.93	8.85
Apr	29.84	28.04	25.12	14.43	21.77	4.61
May	15.38	14.40	13.05	8.18	11.10	2.59
Jun	11.06	10.46	9.53	6.26	8.23	2.02
Jul	8.61	8.12	7.30	4.73	6.31	1.61
Aug	11.57	10.82	9.78	6.55	8.26	2.13
Sep	26.81	25.30	22.71	14.47	19.46	4.67
Oct	42.64	39.25	34.93	21.75	29.58	6.59
Nov	56.32	51.33	45.93	29.21	38.41	8.63
Dec	72.84	67.00	60.53	37.67	50.68	11.43
Annual	40.44	37.19	33.35	20.74	28.11	6.39

Table 3. Mean monthly variability of wind power (W/m^2)

	103	111	112	113	121	122
Jan	2156.11	2146.14	2159.91	1705.97	1980.75	1246.74
Feb	1930.78	1960.01	1946.57	1437.76	1853.22	1090.30
Mar	1682.25	1700.95	1686.49	1257.80	1612.92	949.79
Apr	1067.34	1115.50	1139.02	844.77	1106.67	622.39
May	757.11	794.88	868.11	697.09	796.22	489.40
Jun	657.34	679.89	792.31	684.44	703.47	468.04
Jul	556.03	577.73	632.82	502.32	582.57	351.44
Aug	648.07	667.21	722.05	606.69	645.94	434.43
Sep	1113.20	1149.92	1186.71	939.87	1149.22	746.01
Oct	1502.67	1527.26	1563.79	1215.89	1461.88	934.48
Nov	1714.49	1727.42	1756.67	1386.11	1602.14	1020.92
Dec	1946.14	1985.57	1985.52	1531.97	1896.67	1173.82
Annual	1308.18	1333.17	1367.30	1065.90	1279.89	792.62

Typically, the depth range for fixed offshore wind installations is ≤ 50 m, whereas for the floating ones is between 50 and 1 000 m. Here, as an example, we will examine for the hybrid installations, solutions with depth ≤ 200 m. In Figs. 1–3, grid points situated at depths ≤ 200 m are depicted with red crosses. Among these grid points, those being closer to the coast have been selected for further analysis; see Table 1, where the coordinates and the depth of these points are given.

First, the available wave and wind power resource for these points is evaluated. In Tables 2–3, the mean monthly variability of the wave and wind power is given for the first six of them. Then, the monthly availability (with respect to negative correlation) of these points have been examined. In Table 4, it is shown how many months during the year these points exhibit negative correlation.

Finally, in Fig. 4, those points are depicted with a color scale showing the amount of months as follows: (∘) blue: ≥ 6 (six) months, (∘) orange: < 6 (six) months and ≥ 4 (four) months, (∘) purple: < 4 (four) months and ≥ 1 (one) month. Thus, the blue points (more than 6 months negative correlation) are good candidates for further analysis.

Table 4. Monthly availability (negative correlation)

Point	Months											
	1	2	3	4	5	6	7	8	9	10	11	12
103	✓	✓	✓	✓	✓		✓		✓	✓	✓	✓
111	✓	✓	✓	✓	✓		✓			✓	✓	✓
112	✓	✓	✓	✓	✓		✓			✓	✓	✓
113	✓	✓	✓		✓		✓			✓	✓	✓
121	✓	✓	✓		✓		✓			✓	✓	✓
122	✓	✓	✓		✓		✓			✓	✓	✓
123	✓	✓			✓		✓				✓	
124	✓				✓							
133	✓	✓			✓						✓	
134	✓	✓			✓						✓	
142	✓	✓			✓						✓	
143	✓	✓			✓						✓	
151		✓			✓							
173					✓							
181		✓			✓					✓		
184		✓			✓					✓		
185					✓							
195										✓		

Fig. 4. Points with negative correlation close to the shore, depth ≤200 m (color shows the monthly availability: (a) blue: ≥ 6 months, (b) orange: < 6 months and ≥ 4 months, (c) purple: < 4 months and ≥ 1 month.)

Analysis

Further, the analysis in our study will be focused on point 112, which is closer to the shore and is one of the blue points with negative correlation most of the year (9 months) with good energy yield; see Tables 2–3. In addition, there is no conflict with shooting fields, protected and spawning areas, aquaculture facilities and the marine traffic is mild around it.

The following statistical characteristics of wave and wind power will be evaluated both on annual and monthly basis: 1) Variability analysis 2) Directional analysis 3) Probability analysis Especially, for item 3, the following probability distributions will be calculated: (i) wave and wind power (separately), (ii) significant wave height and wind speed, (iii) wave and wind power (jointly).

Concerning the variability, it exhibits the usual seasonal variation with higher values during the winter, and lower during the summer months. In Fig. 5, the daily variability of both wave and wind power is depicted. The max of the mean value during the winter time is 102 kW/m for wave and 3323 W/m^2 for wind power. Accordingly, during the summer months, the min mean value is 5.4 kW/m for wave and 414 W/m^2 wind power.

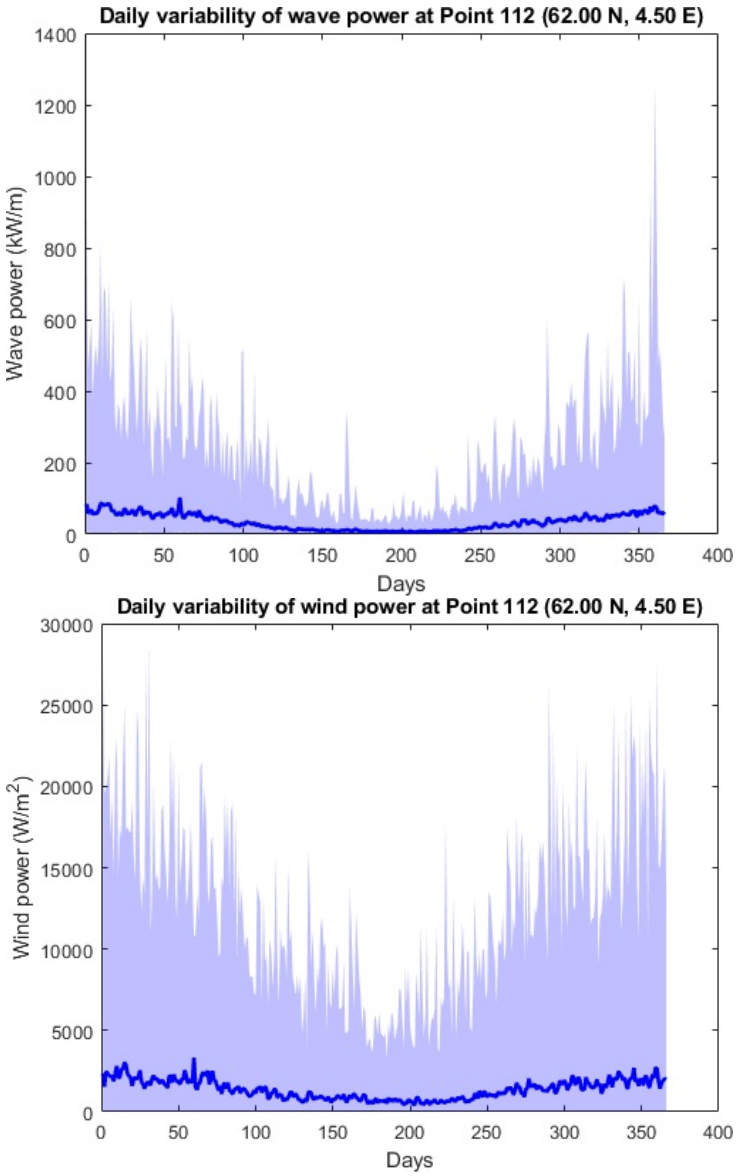

Fig. 5. Daily variability at point 112 (top: wave, bottom: wind power)

It should be also mentioned the high variability in the same season. For example, during winter time, wave power varies between 0 and 1265 kW/m and wind power between 0 and 29188 W/m^2, while in the summer, the wave power variation ranges from 0 to 27 kW/m and wind power from 0 to 3237 W/m^2. Similar results gives also the study of the monthly variability, although the variation is a bit lower since a large amount of data is averaged in comparison with the daily data. For example, for the wave power, max value for the winter monthly variability 1265 kW/m and 120 kW/m for the summer.

Then, directional statistics are derived. The main conclusion is that wave power is always westerly and more distributed than the wind power which is concentrated to northerly and southerly directions. In Fig. 6, wave and wind roses are depicted, based on annual data. The monthly analysis revealed that

the southern direction is prevailing during the winter months (Jan-Mar and Sep-Dec), while during spring/summer months (Apr-Aug) both directions are equally present.

Finally, probability analysis of various quantities has been performed as specified above. In Fig. 7, the joint probability density of significant wave height vs wave energy period together with isolines of wave power are depicted in the top panel. In the bottom panel, the density of wind power is shown, along with the proportional one of wind speed. Monthly histograms have also been derived, omitted here due to space limitations, and are available upon request.

In Fig. 8, the joint histogram of significant wave height vs wind speed is depicted in the top panel, and the the joint histogram of wind and wave power in the bottom panel. The latter is a very useful instrument for the detection of the negative correlation. Since Fig. 8 is based on the annual data, the negative correlation is not so apparent. On the contrary, when one looks at monthly histograms like, e.g., in the bottom panel of Fig. 9, where joint histogram is based on January data, it is more obvious.

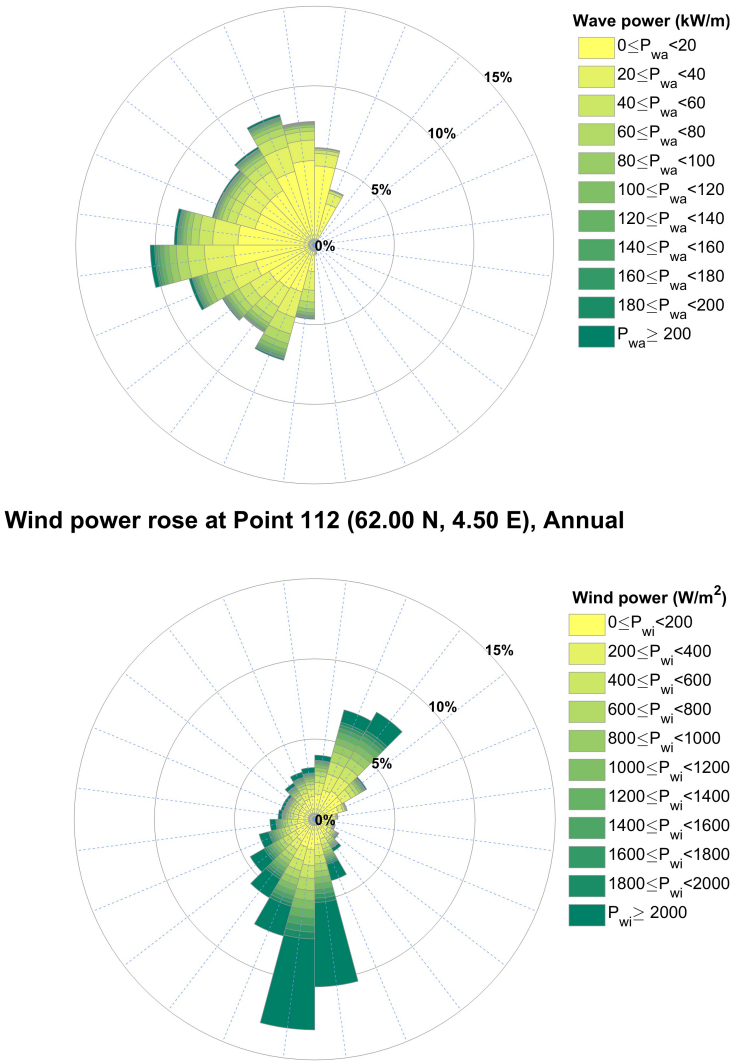

Fig. 6. Directional distribution of wave (top) and wind (bottom) power at point 112. Annual.

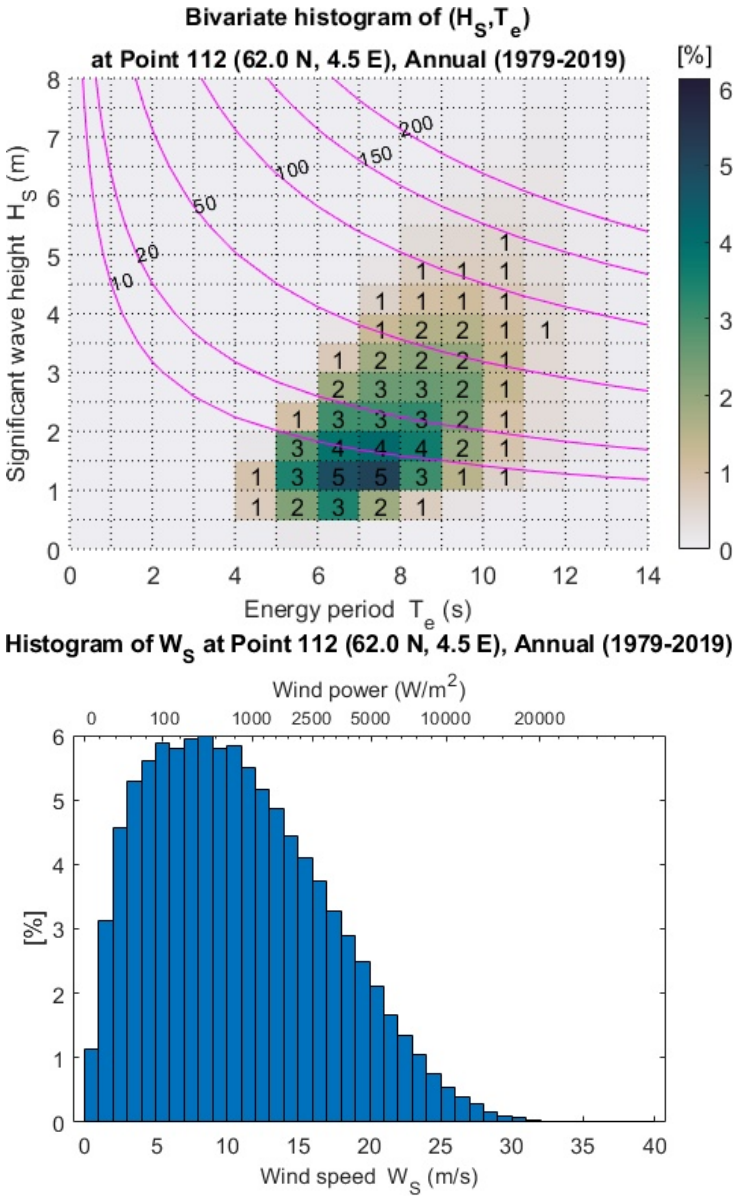

Fig. 7. Probability distribution of wave (top) and wind (bottom) power at point 112. Annual.

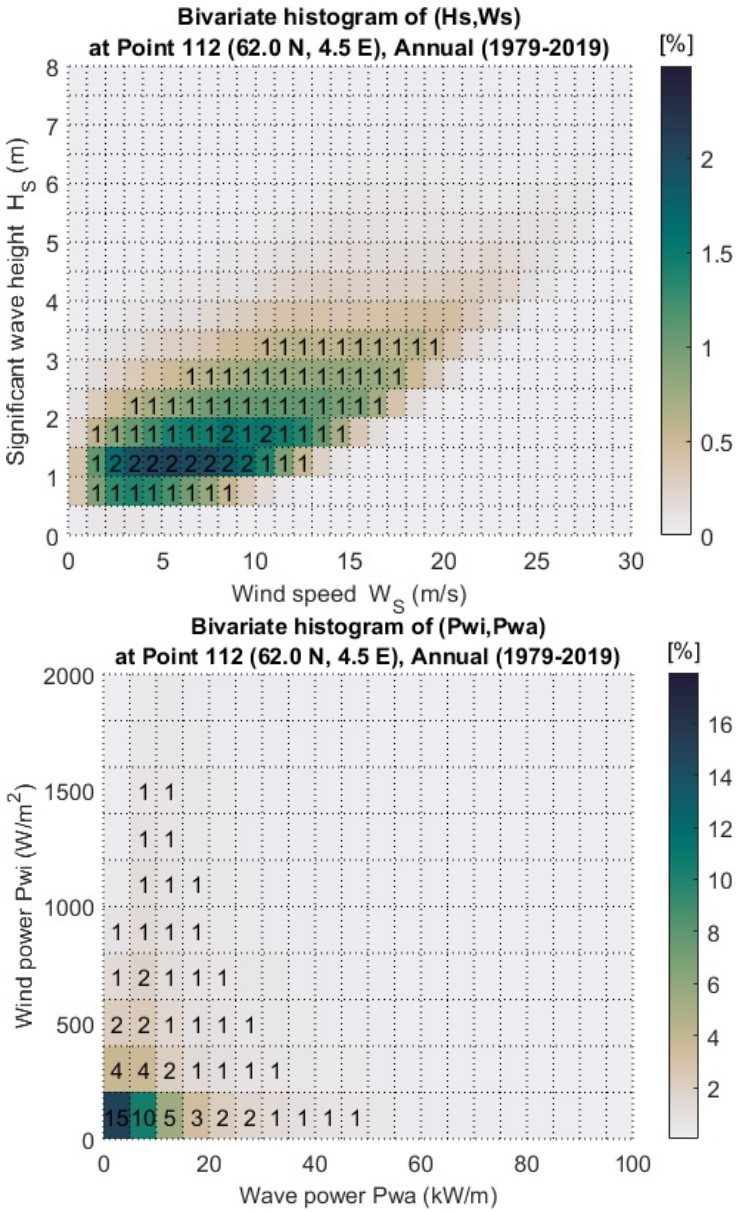

Fig. 8. Joint probability distribution of (a) significant wave height and wind speed (top), and (b) wave and wind power (bottom) at point 112. Annual.

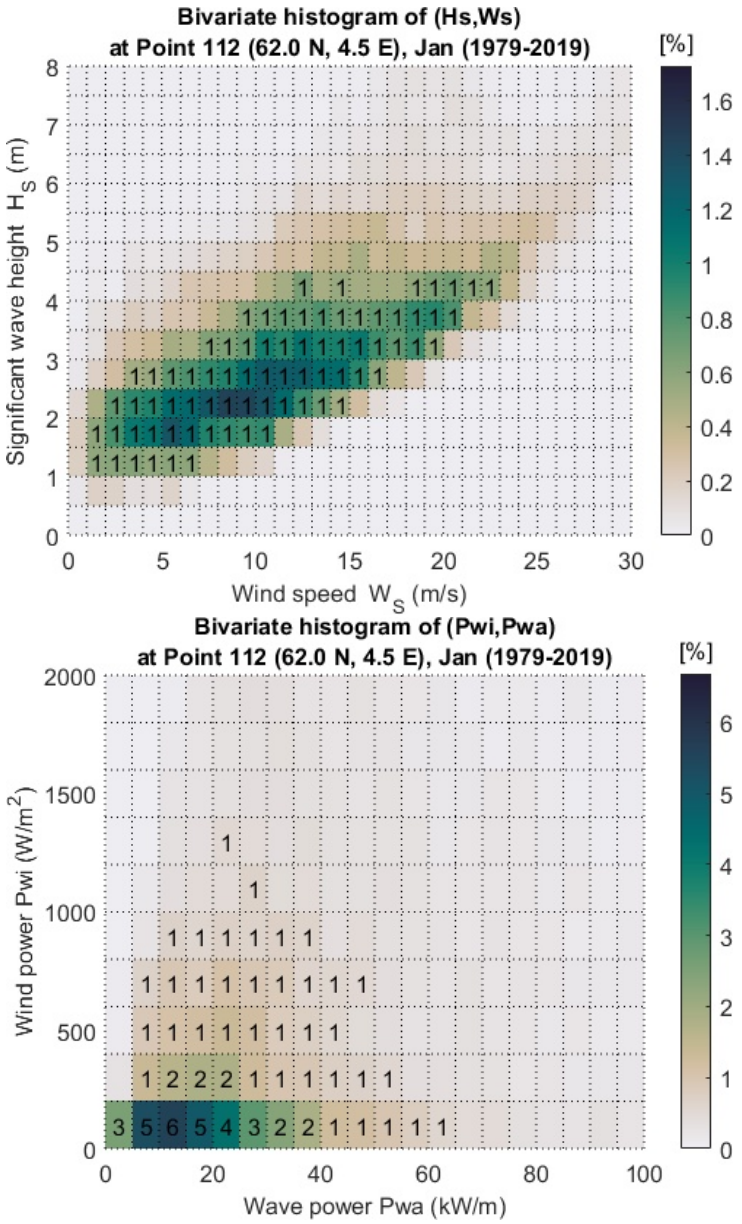

Fig. 9. Joint probability distribution of (a) significant wave height and wind speed (top), and (b) wave and wind power (bottom) at point 112. January.

COMBINED WIND AND WAVE ENERGY PLANT

In this section, a hypothetical example is given of how a combined wave and wind energy plant can be designed, and what energy production can be expected from such a plant. For this, we have to take into consideration the following: (i) Site selection, (ii) Wave & Wind energy converter selection, (iii) Annual energy production.

Site selection

The site should be selected so that the following could be taken into account (Vasileiou et al., 2017): (1) Conflicts with other marine activities: It should not be in direct conflict with other activities in the surrounding marine environment (e.g., shooting fields, protected areas, spawning areas, aquaculture facilities, marine traffic). (2) Distance to shore: The cost of the power plant is likely to increase with distance to shore, in all phases of its lifetime, from installation to daily operation and maintenance. The costs for a cable connection to land and transmission losses, will also increase with distance to shore. These considerations motivate a shorter distance to shore, while both the wave and wind energy resources are likely to be more favourable further away from shore. (3) Connection to local power grid will reduce overall costs.

Based on all the above considerations, site 112 seems a feasible location, appearing not to be in direct conflict with other marine activities, and being intermediate distance from shore at a reasonable depth with exceptional potential wave and wind resources; see also previous section.

Selection of energy conversion systems

Selection of components forming the combined wave and wind power plant design, would typically be driven by minimizing the *Levelized Cost Of Energy* (LCOE), which is the ratio of the sum of costs over the lifetime of the plant to the sum of electrical energy produced over the lifetime of the plant.

The quality of such an optimization process is, thus, directly coupled to the quality of estimates that are made for both costs and energy production. Since this level of detail is beyond the scope of the current investigation, pragmatic assumptions will instead be made to illustrate what could be the result of a detailed LCOE optimization. Namely, (a) nameplate capacity of wind and wave energy conversion systems, (b) efficiency of energy conversion (i.e. capacity factor).

Wind energy. The number of wind turbines required to attain a given farm rating, is dependent on the rated power of the individual wind turbines in the wind farm. For the sake of simplicity (and in line with standard practice for existing large-scale commercial wind farms) it is assumed that all turbines in a wind farm are of the same type.

Defining the exact turbine layout within a wind farm is beyond the scope of this investigation. For the sake of simplicity, a rectangular farm layout with staggered rows is assumed (Archer et al., 2013). A rectangle with a target aspect ratio 2 is used as baseline - columns extend down the length of the short side, and rows along the long side. Furthermore, it is assumed that within a row, turbines are spaced 6 rotor diameters apart, while within a column, wind turbines are spaced 8 rotor diameters apart. Finally, it is assumed that consecutive rows of turbines are staggered with respect to each other by half the intercolumn spacing, i.e. 3 rotor diameters.

For the purpose of this case study, an intermediate sized offshore wind farm with nameplate capacity of approximately 400 MW is selected. Following current trends for offshore wind farms favouring larger turbines (supported by being the turbine with the highest average capacity factor at sites considered) the IEA 15 MW wind turbine is selected as wind turbine model. This implies a wind farm with 27 IEA 15 MW wind turbines, for a total nameplate capacity of 405 MW.

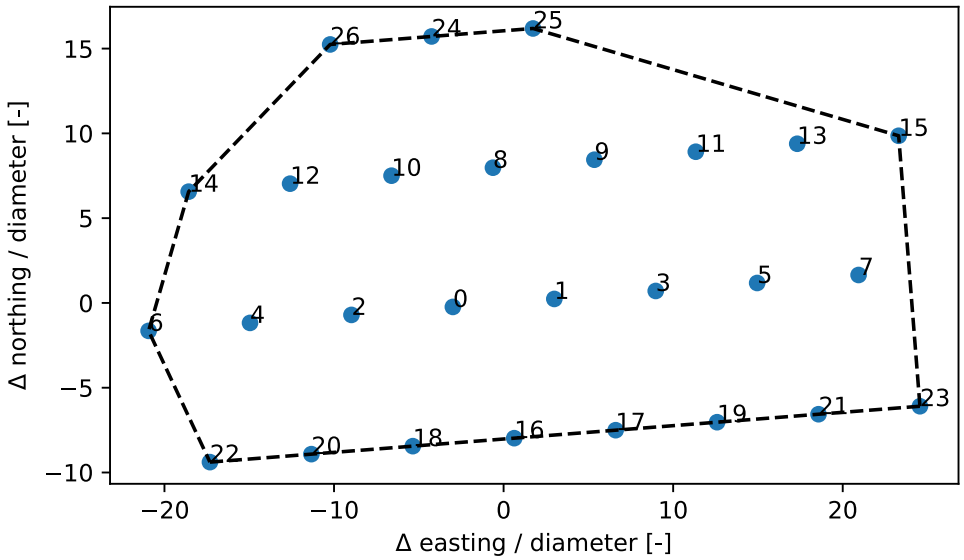

Fig. 10. Layout of a 405 MW wind farm at site 112. Markers indicate the assumed location of wind turbines. The 1566 wave energy converters will be evenly distributed within the footprint of the wind farm.

The layout of the wind farm is determined based on pragmatic choices for inter turbine spacing, and the orientation of the wind farm was adjusted to minimize wake losses taking based on local wind conditions for site 112; see Fig. 10.

Thus, the procedure can be summarized as follows:

- Select a wind turbine model by determining
  - power conversion performance and rotor thrust curves,
  - rotor diameter,
  - hub height.
- Determine farm layout given rotor diameter and selected inter turbine spacing.
- Convert wind speed data form reference height to hub height, assuming the IEC normal wind profile with shear coefficient α=0.14; see International Electrotechnical Commission (2019, section 6.4.3.2):

$$v(z) = v_{ref}\left(\frac{z}{z_{ref}}\right)^{\alpha} \tag{2}$$

  In a more detailed study, one may want to replace this assumed constant value for α with a fit to the hourly ERA5 data at different elevations. Given that the reference height for the available data is z_{ref} = 100 m, Eq. 2 is used to transform tabulated values of v_{ref} to hub height values of the different wind turbines, before looking up generator power.
- Distribute the hourly history from 1979 to 2019 of hub height wind speed and direction into bins, and determine frequency of occurrence of wind speed & direction combinations for an average year.
- Determine the optimal orientation of the wind farm layout at the selected location:

- For a given orientation of the wind farm, simulate power production for all wind speed and direction combinations to determine the Annual Energy Production (AEP). The downstream influence of wind turbine wakes are accounted for as described in Stanley and Ning (2019), where wake velocity deficit is determined by rotor thrust and downstream separation.
- Repeat the previous operation for a range of wind farm orientations.
- Select the farm orientation that results in the largest AEP.

Wave energy. The area available for wave converter installation is assumed to be given by the dimensions of the wind farm. Based on the dimensions of the considered units, and assuming equidistant spacing, estimates are made for a number of wave energy converters of a particular kind that will fit into the wind farm area. The WECs selected for this study are given in Table 5. In the same table, the rated power of the Power-Take-Off (PTO) of the specific version of the WECs considered is listed, along with the source of information used. The selected WECs cover most of the WEC archetypes known in the available literature.

The wave energy output from the different WECs was estimated using their power matrices published in the listed sources, see Table 5, together with the selected site(s) monthly/yearly wave scatter diagram(s). The wave scatter diagrams are expressed in pairs of H_S and T_e. Therefore, the relation $T_e = 0.9T_p$ was used (Ahn, 2021) for the cases where the power matrix is published in pairs of peak period T_p and H_S and a JONSWAP spectral shape with peak enhancement factor equal to 3.3 being assumed.

Table 5. Selected WECs.

Name	Description	P_{rated} [kW]	Source
AquaBuOY	Self-reacting heave point absorber	250	Silva et al. (2013)
OEbuoy	Floating oscillating water column	2900	Bento et al. (2018)
Oyster	Shallow Water surging terminator	315	Silva et al. (2013)
Pelamis	Semi-submerged articulated attenuator	750	Silva et al. (2013)
RM3	Two-body heave point absorber	N/A	Neary et al. (2014)
Wave Dragon	Floating Overtopping	7000	Bento et al. (2018)

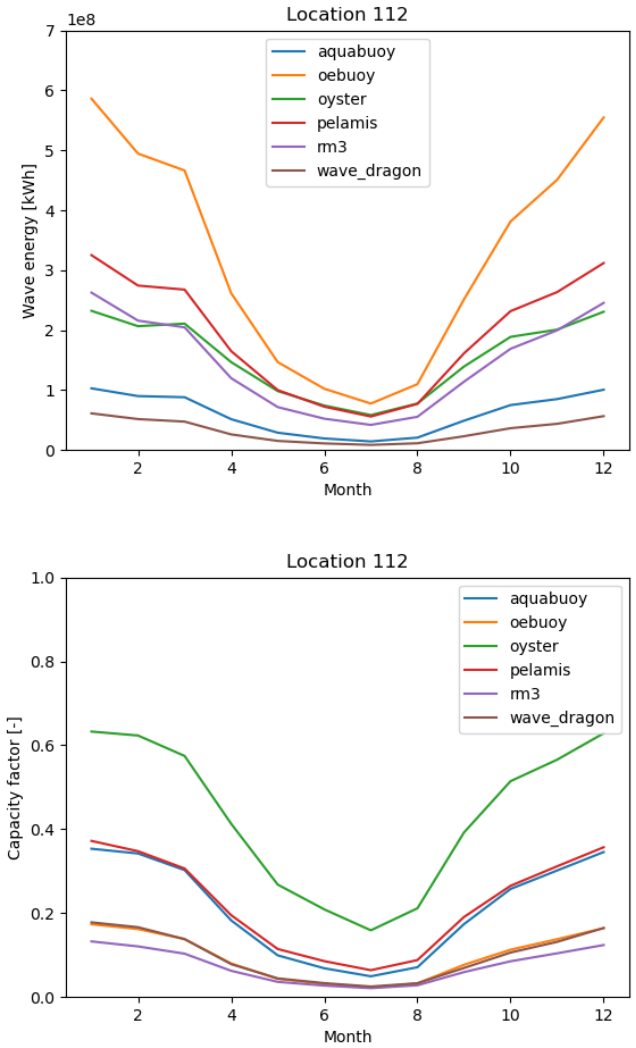

Fig. 11. Monthly variation of Energy Production (top) and Capacity Factor (bottom) of WECs at site 112.

The power matrices were used directly from the listed sources and one assumes that factors such as survival modes in extreme sea states are included to some extent. Except for the RM3 device, this appears to be the case; although no further investigation was carried out in this respect.

No hydrodynamic interactions between WECs in the farm are accounted for in the procedure described. An (arguable) reasonable spacing between WECs of 1 000 m, for the Wave Dragon, and 200 m for the other devices was used, assuming that this will substantially reduce interactions.

Given a lack of other detailed metrics to base a decision on, the wave energy converter model is chosen based on estimated annual Energy Production (EP) and capacity factor (CF). The model with the highest CF at site 112 is the Oyster; see Fig. 11, bottom panel. However, this is not suitable for the water depth of the site. Given its relatively high CF and EP characteristics (see Fig. 11, top panel), the AquabuOY is selected as wave energy converter for the hypothetical combined wave and wind farm. This implies a wave farm with 1566 AquabuOY wave energy converters of 250 kW each, for a nameplate capacity of 391.5 MW.

The large number of WECs is a result of the choice of a single metric, CF, together with the limited set of WEC designs considered in the analysis. In real applications, the WEC design should be adjusted to the specific site conditions, including the PTO rated power, especially when a large number is to be manufactured and deployed. Furthermore, a comprehensive techno-economic analysis should be carried out, which would probably reduce the attractiveness of such a high number of WECs and favour other designs (e.g., from including power-cables and mooring systems related costs into the equation).

Annual energy production

Once the location, as well as wave- and wind energy converters have been selected, metocean data for the selected site over a period stretching from 1979 to 2019 is used as input to estimate energy production from the hypothetical combined plant for an average year, equivalent to 8760 hours of operation. Capacity factor is determined by dividing the calculated energy production given local conditions by 8760 $\times$ the rated energy production of the wave-, wind- or combined farms, respectively.

Fig. 12, top, shows that, although there is seasonal variation in both wave and wind energy generated, the variation is largest for wave energy. More energy is converted (more efficiently) during the winter months of the year. Table 6 summarizes the annual energy production from the plant.

Table 6. Annual energy production (AEP) and capacity factor (CF) of the combined wave and wind farm.

source	AEP [kW h]	CF [-]
Wind	2.396×10^9	0.675
Wave	7.255×10^8	0.212
Combined	3.121×10^9	0.447

Effects of combining wave- and wind energy production

As alluded as early as in the title, the objective of this investigation was to quantify any beneficial influence of observed negative correlation between available wave- and wind energy. It is believed that this negative correlation will lead to less variability in the total converted energy for a combined wave- and wind farm, as opposed to either of these technologies working in isolation.

To further investigate this, we consider the estimated hourly energy production over a monthly period for the previously defined hypothetical combined wave and wind farm. Fig. 9, for example, indicates negative correlation between available wind and wave energy during the month of January at site 112.

Time series of hourly energy production for January 2000 are shown in Figs. 13 (blue line in top and middle panel and green in bottom panel). In addition, time series of significant wave height and peak wave period are plotted in top panel of Fig. 13, and wind speed, cut-in/out and the rated production in middle panel.

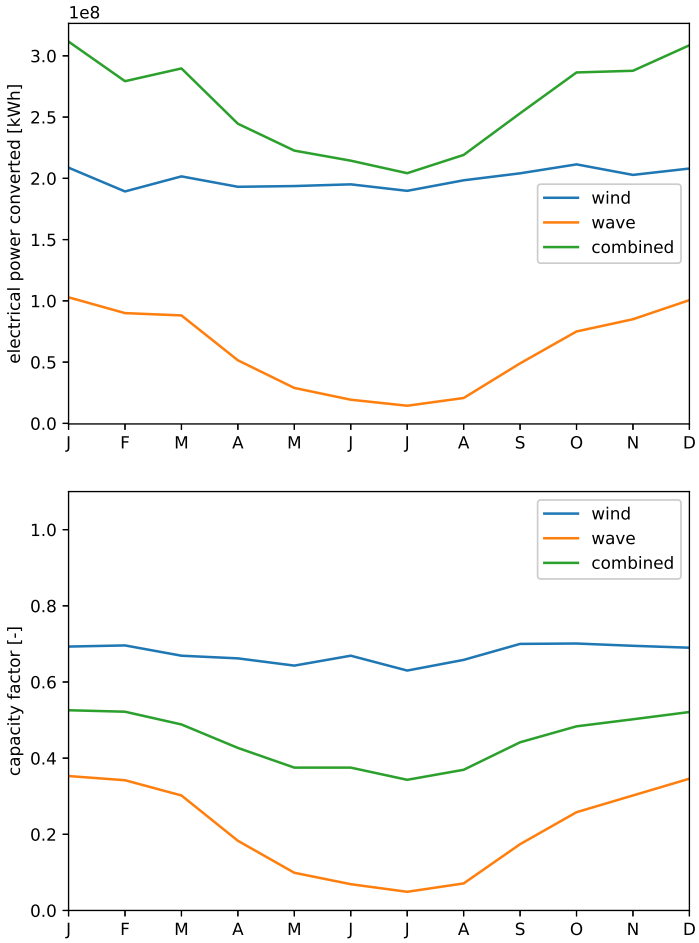

Fig. 12. Averaged monthly variation of Energy Production (top) and Capacity Factor (bottom) from the combined wave and wind farm at site 112.

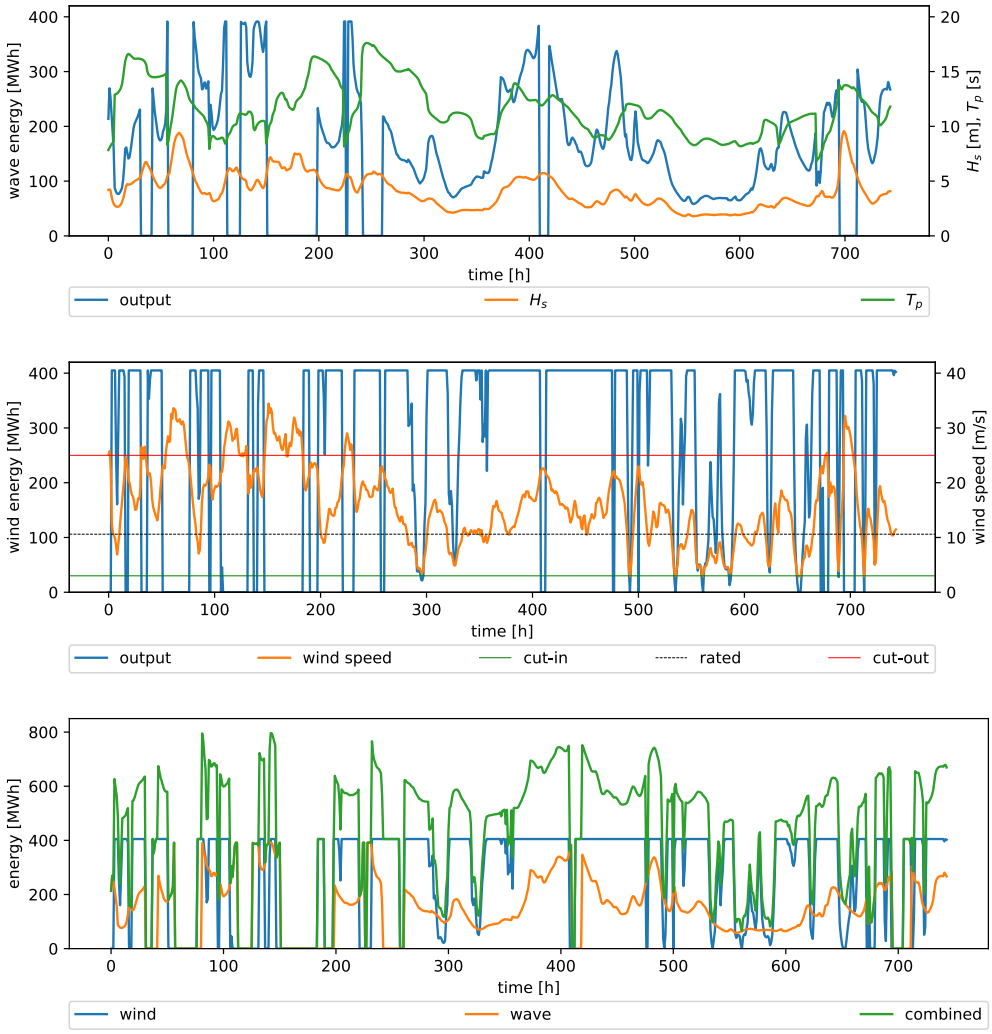

Fig. 13. Environmental conditions at location 112 during the month of January 2000, and estimated hourly wave, wind and combined farm output.

The wind farm production reaches rated value for large proportions of time, although it is also stopped at times where wind speed becomes either lower than the cut-in or higher than the cut-out speed. The stoppages due to too high wind speeds frequently coincide with stoppages in wave energy production due to too harsh wave conditions.

In the bottom panel of Fig. 13, where the total energy production is plotted (together with wave and wind production, separately), the varying nature of the power production is apparent. A fact that is attributed to the substantial variability of both time series of estimated wave and wind production.

In any case, and despite this varying nature, Table 7 indicates that the RMS (scaled with mean) for the combined wave and wind farm is lower than the corresponding value when only one (either wave or wind) farm is operating.

Table 7. Mean and root mean square (RMS) of hourly energy production during January 2000 at site 112 for a combined wave- and wind farm.

	mean [MW h]	rms [MW h]	rms/mean
wind	273.114	324.860	1.189
wave	147.443	182.030	1.235
combined	420.557	479.171	1.139

CONCLUDING REMARKS

In the present work, an academic case-study scenario has been worked out for the investigation of a combined wind and wave farm at the Norwegian waters. This initiated from the finding of offshore areas in the Norwegian waters with negative correlation between wind and wave energy, which in turn suggests an efficient way of combination of these two energy sources.

For this study, the latest ECMWF's wind and wave database, ERA5, have been used for the resource evaluation of offshore wind and wave power. The database has a very good spatial (0.5°×0.5°) and temporal coverage (1979-2019). Also, for the power resource evaluation, direct use of mean energy period and wind speed at 100 m height is made for the first time, instead of using empirical approximations based on relations with peak period and wind speed at 10 m, respectively.

Metrics such as the yearly absorbed power and its annual variation have been analyzed. Different wind/wave energy converter types with published/state-of-the-art power matrices have been used for the estimation of hourly absorbed energy throughout the entire period covered by the ERA5 database.

The procedure showed that the combined use of the two energy resources is favourable than the use of each one separately.

The described procedure would potentially establish a working methodology for easily assessing the potential of marine wind and wave renewable devices at early stages of development.

ACKNOWLEDGMENTS

The work in this paper has been funded by internal basic funds (PFO Fornybar energi) of SINTEF Ocean, which are gratefully acknowledged.

REFERENCES

Ahn S (2021). "Modeling mean relation between peak period and energy period of ocean surface wave systems," *Ocean Engineering*, 228, 108937.

Archer CL, Mirzaeisefat S, and Lee S (2013). "Quantifying the sensitivity of wind farm performance to array layout options using large-eddy simulation," *Geophysical Research Letters*, 40(18), 4963–4970.

Astariz S and Iglesias G (2016a). "Selecting optimum locations for co-located wave and wind energy farms. part i: The co-location feasibility index," *Energy Conversion and Management*, 122, 589–598.

Astariz S and Iglesias G (2016b). "Selecting optimum locations for co-located wave and wind energy farms. part ii: A case study," *Energy Conversion and Management*, 122, 599–608.

Bento AR, Martinho P, and Soares CG (2018). "Wave energy assessement for northern spain from a 33-year hindcast," *Renewable Energy*, 127, 322–333.

Cozzi L, Ferroukhi R, Souza L, et al. (2022). *Tracking SDG7. The energy progress report 2022*, Technical report, IEA, IRENA, UNSD, World Bank and WHO.

Gaughan E and Fitzgerald B (2020). "An assessment of the potential for co-located offshore wind and wave farms in ireland," *Energy*, 200, 117526.

Hersbach H, Bell B, Berrisford P, et al. (2020). "The ERA5 global reanalysis," *Quarterly Journal of the Royal Meteorological Society*, 146(730), 1999–2049.

International Electrotechnical Commission (2019). "Wind energy generation systems - part 3-1: Design requirements for fixed offshore wind turbines," *IEC 61400 3 12019*.

McTiernan KL and Sharman KT (2020). "Review of hybrid offshore wind and wave energy systems," *Journal of Physics Conference Series*, 1452(1), 012016.

Neary VS, Lawson M, Previsic M, et al. (2014). "Methodology for design and economic analysis of marine energy conversion (MEC) technologies," *SANDIA REPORT SAND2014 9040*.

Pérez-Collazo C, Greaves D, and Iglesias G (2015). "A review of combined wave and offshore wind energy," *Renewable and Sustainable Energy Reviews*, 42, 141–153.

Rosa-Santos P, Taveira-Pinto F, López M, and Rodríguez CA (2022). "Hybrid systems for marine energy harvesting," *Journal of Marine Science and Engineering*, 10(5).

Silva D, Rusu E, and Soares C (2013). "Evaluation of various technologies for wave energy conversion in the portuguese nearshore," *Energies*, 6(3), 1344–1364.

Stanley APJ and Ning A (2019). "Massive simplification of the wind farm layout optimization problem," *Wind Energy Science*, 4(4), 663–676.

Stefanakos C, Tedeschi E, and Brönner U (2021). "Offshore wind and wave energy resource assessment in the Norwegian waters based on ERA5 reanalysis," in *31th International Offshore and Polar Engineering Conference, ISOPE'2021*, Rhodes, Greece, pp. 651–658.

Vasileiou M, Loukogeorgaki E, and Vagiona DG (2017). "GIS-based multi-criteria decision analysis for site selection of hybrid offshore wind and wave energy systems in Greece," *Renewable and Sustainable Energy Reviews*, 73, 745–757.